Gastro Hep Advances 2024;3:954–964

ORIGINAL RESEARCH—BASIC

Glucagon-Like-Peptide-2 Stimulates Lacteal Contractility and Enhances Chylomicron Transport in the Presence of an Intact Enteric Nervous System

Majid Mufaqam Syed-Abdul,[1,*] Lili Tian,[1,*] Timothy Samuel,[2,3] Alex Wong,[4] Young-Kwon Hong,[4,5] Ralph S. Dacosta,[2,3] and Gary F. Lewis[1,†]

[1]Division of Endocrinology, Department of Medicine and Physiology, University of Toronto, Toronto, Ontario, Canada; [2]Princess Margaret Cancer Centre, University Health Network, Toronto, Ontario, Canada; [3]Department of Medical Biophysics, University of Toronto, Toronto, Ontario, Canada; [4]Division of Plastic and Reconstructive Surgery, Department of Surgery, Keck School of Medicine, University of Southern California, Los Angeles, California; and [5]Department of Biochemistry and Molecular Medicine, Norris Comprehensive Cancer Center, Keck School of Medicine, University of Southern California, Los Angeles, California

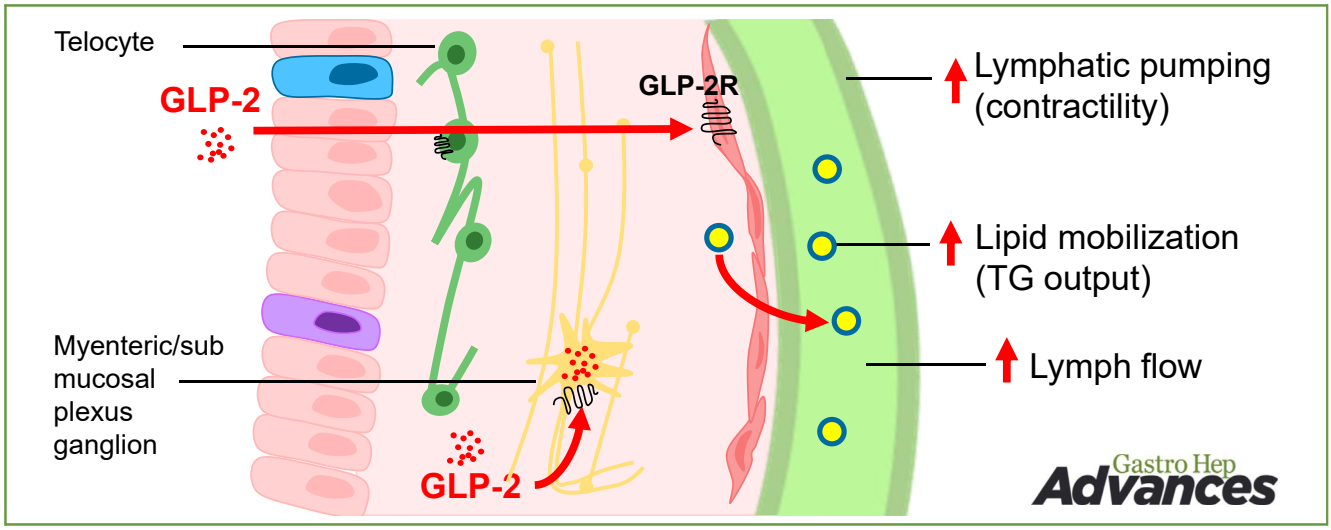

BACKGROUND AND AIMS: Secretion and transport of intestinal chylomicrons (CMs) via lymphatics to the blood circulation is stimulated primarily by fat ingestion, whereas several other factors have also been shown to play important roles in regulating CM secretion rate. Among these factors, active regulation of lymphatic pumping has not been appreciated to date. The gut peptide and intestinal growth factor glucagon-like peptide-2 (GLP-2) has emerged as a robust enhancer of intestinal lipid mobilization and secretion. The present study aims to elucidate GLP-2's impact on lacteal contractility and assess enteric nervous system (ENS) involvement in GLP-2–induced effects on lipid mobilization. **METHODS:** Using intravital imaging of a prospero-related homeobox 1-enhanced green fluorescent protein rat model, we assessed GLP-2's effect on lacteal contractility, in the presence and absence of the ENS inhibitor mecamylamine (MEC). Concurrently, to explore the physiological relevance, we examined GLP-2's impact on lymph flow and triglyceride (TG) output in vivo in a rat lymph fistula model. **RESULTS:** GLP-2 significantly increased lacteal contractility, and this effect was inhibited by MEC. In the rat lymph fistula model, GLP-2 increased lymph flow, lymph volume, cumulative lymph volume, and TG output while reducing lymph TG concentration. MEC administration blocked these effects of GLP-2. Peak enhancement of lacteal contractility and enhancement of lymph flow *in vivo* occurred simultaneously with maximal effect at 15–20 minutes post GLP-2 administration, suggesting that GLP-2 enhances lipid transport by stimulating lymphatic contractility. **CONCLUSION:** For the first time, through imaging and concurrent rat lymphatic fistula studies, we demonstrated active regulation of lymphatic contractility as a key determinant of CM secretion and that intact ENS was required to observe this effect.

Keywords: GLP-2; Lymphatic Pumping; Intravital Imaging; Chylomicron Secretion

*Shared first co-authors. †Lead contact.

Abbreviations used in this paper: **apoB48, apolipoprotein B48; AUC, area under the curve; CM, chylomicron; EGFP, enhanced green fluorescent protein; ENS, enteric nervous system; GLP-2, glucagon-like peptide-2; LP, lamina propria; MATLAB, Matrix laboratory; MEC, mecamylamine; nNOS, neuronal nitric oxide synthase; PBS, phosphate buffered saline; Prox1, prospero-related homeobox 1; TG, triglyceride.**

Most current article

2772-5723
https://doi.org/10.1016/j.gastha.2024.06.009

Introduction

Intestinally derived remnant lipoproteins are atherogenic and have long been considered a therapeutic target for the prevention of cardiovascular disease.[1] Chylomicron (CM) secretion by the intestine is stimulated primarily by fat ingestion, with a second-order, fine regulation by systemic and local factors including nutrients, nutraceuticals, hormones, and neural networks.[2] Whereas enterocyte CM assembly, maturation, and secretory pathways have been investigated extensively for several decades, the contribution of extracellular transport mechanisms, such as lymphatic pumping, to CM appearance in blood circulation has not been appreciated to date.

Of several regulators of CM secretion, we have identified glucagon-like peptide-2 (GLP-2) as a potent mobilizer of intestinal lipid,[3] acutely enhancing preformed CM release from the intestine in humans,[4,5] and animal models,[6,7] when administered at pharmacological doses. Its effect on CM secretion is rapid (first occurring within 10–15 minutes), independent of fat ingestion, robust, and reproducible in humans and animals. In a study conducted by Grande et al,[8,9] GLP-2 appears to act through the neuronal nitric oxide synthase–generated nitric oxide to induce its effects on lipid absorption and CM production in mouse and hamster models. However, in our human study,[5] inhibition of nitric oxide synthase did not impair GLP-2–mediated intestinal lipid mobilization despite inhibition of intestinal blood flow, calling into question the role of NO in mediating GLP-2's effect on lipid mobilization in humans. Additionally, in several studies, we have previously shown that GLP-2 rapidly mobilizes preformed CMs residing in intestinal lipid storage compartments, likely either in the lamina propria (LP) or in the lymphatic circulation.[4–7] First, in a tracer-kinetic study in healthy humans, we showed that a single dose of GLP-2 administered 7 hours after ingestion of a high-fat liquid formula rapidly increased preformed CM appearance in human plasma, rather than enhanced synthesis of newly formed lipoprotein particles, within 30 minutes and reached a peak in the blood circulation at 1 hour.[4] Second, transmission electron microscopy of human duodenal tissue collected 1 hour after GLP-2 or placebo administration and 6 hours after a high-fat drink showed no detectable differences between GLP-2 or placebo on cytoplasmic lipid droplet size, number, and total area suggesting no mobilization of intracellular lipid pools.[10] However, despite this lack of effect on intracellular lipid stores, GLP-2 robustly increased plasma triglyceride (TG) in CM-sized lipoproteins.[10] In accordance with this, disruption of Golgi function by Brefeldin A in mesenteric lymph cannulated rats did not affect GLP-2–mediated mobilization of intestinal lipid stores, suggesting that GLP-2 acts distal to the Golgi, a distal intracellular step in CM maturation and secretion.[7]

Furthermore, we have also demonstrated that antagonism of the GLP-2 receptor (GLP-2R) blunts its ability to stimulate lymph flow.[7] Since GLP-2Rs are not expressed on enterocytes but are abundant on subepithelial myofibroblasts and enteric neurons[11] as well as vagal afferent neurons[12] found within subepithelial regions of the intestine, including the LP. This observation provides further support to the notion that GLP-2 acts primarily extracellularly. Finally, intraperitoneal GLP-2 administered 5 hours after an intraduodenal lipid bolus rapidly and robustly increased mesenteric lymph flow and apolipoprotein B48 appearance in rats, without changing the size of CM particles.[6] The lack of effect on CM lipidation points to the mobilization of extracellular preformed CMs, perhaps within the LP or mesenteric lymphatics. Therefore, GLP-2 provides a unique tool to explore the regulation of lymphatic pumping (lacteal contractility) and its contribution to CM appearance in blood circulation.

Lacteal contractility has been shown to be partly regulated through the enteric nervous system (ENS).[13,14] Therefore, in this study, we reasoned that if blockade of the ENS blocks GLP-2's enhancement of lymph flow, it would provide additional evidence that GLP-2 may be regulating its lipid-mobilizing effect by stimulating lacteal contractility.

In the prospero-related homeobox 1 (Prox1)-enhanced green fluorescent protein (EGFP) rat model and rat lymph fistula model, for the first time, we have demonstrated that GLP-2 enhances lacteal contractility, in the identical time frame to its effect on intestinal lymph flow and lymphatic TG output, and furthermore, we demonstrated that this effect is completely abolished by blockade of the ENS. These studies demonstrate for the first time that the rate of CM transport to the blood circulation is determined in part by active regulation of lymphatic contractility, which must be considered along with regulation of intestinal lipid absorption, CM assembly, and secretion by enterocytes when considering CM production rate. Furthermore, partial blockade of lymphatic contractility may be a novel pharmacological target to slow potentially atherogenic CM delivery from the gut to the circulation, thereby limiting the postprandial excursion of potentially atherogenic lipoproteins in the blood circulation.

Methods

Animals

All the animal procedures were approved by the University Health Network Animal Care Committee (Approval #5690, #6211).

Prox1-EGFP rat model. The Prox1-EGFP rat was developed and generously gifted by Dr Young-Kwon Hong from the University of Southern California. This model is a bacterial artificial chromosome–based lymphatic reporter rat, where EGFP is expressed under the regulation of the Prox1 promoter, and has been used to conveniently visualize lymphatic vessels and other Prox1-expressing tissues. This model has been demonstrated to have completely normal mesenteric lymphatic contractile function.[15] The rats were maintained in colonies at the University Health Network-approved facilities. Only rats with Prox1-EGFP positive (confirmed via presence of green luminance in eyes, checked using ultraviolet [UV] light) were included in the study.

Rats that were Prox1-EGFP negative were not used due to technical challenges of laminating lacteal under the microscope. The primary advantage of using a transgenic rat model over administering imaging dyes resides in the consistent maintenance of imaging intensity throughout the time-series videos, as opposed to dyes that exhibit gradual depletion over time. At birth, rats were tested for Prox1 positivity by checking the green color in the eyes illuminated under the UV light. Six–8-week-old rats were used for imaging experiments.

Sprague-Dawley rats. Male Sprague-Dawley rats (Envigo Laboratories, Indianapolis, IN) were maintained with a 12-hour light/dark cycle and free access to water at the Animal Resources Centre of the University Health Network. Six–8-week-old rats were used for lymph cannulation studies.

Study Design

Figure 1A represents the experimental protocol for lacteal contractility studies (intravital imaging) and Figure 1B represents the experimental protocol for rat lymph fistula model studies (lymph duct cannulation).

Intravital fluorescence imaging. Intravital fluorescence imaging is a powerful tool that has provided new insights into basic research and its utility has been expanding.[16] The technique has been used for investigating various tissues either transdermally (nonsurgical) such as blood vessels in the skin or deep tissues (surgical) such as visceral, vital organs, and intestines using a myriad of techniques to access them.[16] Despite its potential, there has been a notable gap in studying the contractility of lacteals. A single study[14] conducted in 2015 demonstrated this phenomenon; yet surprisingly, no follow-up studies were published by the same research group or others using similar techniques. Additionally, because of the lack of published experimental details on which to replicate methods and the lack of clarity of published data, we developed our own technique to quantify changes in lacteal diameter as a surrogate for lacteal contractility.

Surgical protocol. Briefly, a live, anesthetized rat (previously deprived of food for 16 hours) was placed on a custom 3-dimensional printed stage designed using Fusion 360 Software (V.2.0.13619, Autodesk Inc, Toronto, ON). Under continuous general anesthesia (Isoflurane Vaporizer), approximately 10–12 cm of the rat's proximal jejunum was exteriorized and placed on a chamber filled with saline-wet gauze to maintain the vitality of the tissue (Figure 1A, TOP VIEW and Figure A1A). About 1.5 cm of the jejunum was incised horizontally along the

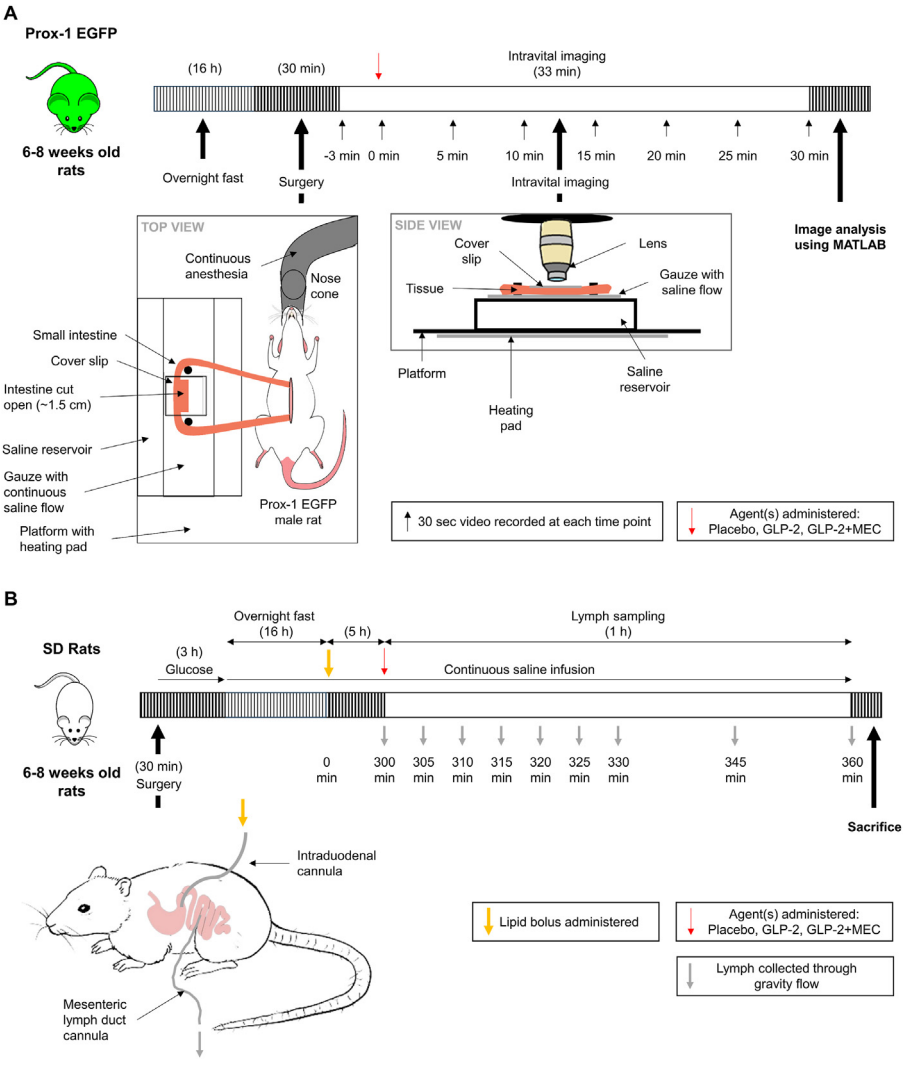

Figure 1. Study design for intravital imaging protocol and rat fistula studies. (A) Study timeline for the intravital imaging protocol. Detailed surgical procedures are provided in the "top view" and the "side view" sections. (B) Study timeline for the rat lymph fistula model. GLP-2, glucagon-like peptide 2; MEC, mecamylamine.

antimesenteric border. The exposed intestinal lumen was cleaned with a saline-moistened swab to remove any debris and was stabilized by using a coverslip. The prepared section was placed under the 2-photon confocal microscope to visualize the lacteals in the villi using 5x lens (to locate the lacteals) and 40x lens (to record the lacteal contractility) (Figure 1A, SIDE VIEW).

Pharmacological treatments. As shown in Figure 1A, Prox1-EGFP rats received one of the following treatments.

- Placebo: Saline administered intraperitoneally within 15 seconds immediately before time point 0 (discussed below in imaging protocol), to assess the effect on lacteal contractility. n = 8 rats were used for this group.
- GLP-2: GLP-2 was synthesized as dipeptidyl peptidase 4–resistant analog [Gly2]-GLP-2 by Pepceuticals, Inc and was tested for purity using reverse phase analytical high-performance liquid chromatography and/or by matrix-assisted laser desorption/ionization mass spectrometry (> 90% purity) using a robust QC system that was ISO9001:2008 (British Standards Institution) accredited (Pepceuticals, Inc, Leicestershire, UK).[7] GLP-2 (75 μg) was diluted in 0.5 mL phosphate buffered saline (PBS) and was administered intraperitoneally within 15 seconds immediately before time point 0. n = 8 rats were used for this group.
- GLP-2 + mecamylamine (MEC) (ENS inhibitor): During the imaging protocol (discussed below), MEC (10 mg/kg body weight) was administered intraperitoneally followed by GLP-2 (75 μg of GLP-2 in 0.5 mL PBS) administration within 30 seconds time frame immediately before time point 0 minute. n = 8 rats were used for this group.

Two-photon intravital microscopy for lacteal in situ imaging. A 2-photon confocal fluorescence microscope was used to visualize lacteals by exciting the GFP using a 930-nm laser. Intestinal villi were located using a FLUAR 5x/0.25 dry lens (working distance of 12.5 mm) and the Plan-Apochromat 20x/1.0 DIC (UV) VIS-IR wet lens (water-based with a working distance of 1.7 mm) was used for the acquisition of final videos, at the rate of 120 frames per minute (the quality of videos was distorted above this rate; therefore, we collected videos at 2 frames per second). This working distance was maintained as a precaution to prevent the undulations of the immersion lens could lead to unexpected contractions, as the tension on the tissue can be influenced by the undulating z-positioning of the lens. As shown in Figure 1A, first, a 30-second baseline video was recorded at a time point 3 minutes prior to starting the experiment (−3 minutes) to quantify baseline variation (regular breathing) in the lacteal diameter and to control for background noise. Videos longer than 30 seconds resulted in photobleaching and tissue damage; therefore, videos at each time interval were recorded for 30 seconds. Moreover, data collected over 30 seconds during each time point were sufficient to capture lacteal contractility. Next, it is important to note that while the previous published study[14] administered treatments superficially or directly on the tissue, we chose to administer them intraperitoneally (as represented by a red arrow in Figure 1A) due to its greater physiological relevance. Post agent administration, subsequent 30-second video clips were recorded at the following time points: 5 minutes, 10 minutes, 15 minutes, 20 minutes, 25 minutes, and 30 minutes.

Matrix laboratory quantification protocol. Once the images and time-lapse videos were captured, a custom-written Matrix laboratory (MATLAB) script (vR2021A, The MathWorks, Inc, Natick, MA, United States) was used to analyze and quantify the contractility or changes in the diameter of the lacteal,[14] in response to test agents. It is noteworthy that the preceding investigation[14] used various filters and image-rendering algorithms to correct for potential artifacts. The data presented by these investigators underwent multiple corrections. However, the MATLAB codes used therein were not publicly accessible for our utilization. Therefore, we developed a basic code employing a publicly available MATLAB script to quantify alterations in lacteal diameter. The alteration in lacteal diameter was quantified by tracing a horizontal line across the lacteal, commencing from the nonlacteal region (background), traversing through the lacteal, and ending back in the nonlacteal area (background), as presented in Figure A1B. Recognizing the asymmetry of lacteal diameter depending upon the region of interest, we captured lacteal diameter at 5 different regions to remove any artifacts. Thus, for this analysis, 5-line profiles were randomly drawn at various locations along the lacteal, and the mean of these line profiles was presented (Figure A1B). The superiority of employing 5-line profiles over a single-line profile lies in its capacity to attenuate noise within a particular region of the lacteal. Raw data associated with the 5-line profiles were exported to an MS Excel file, and were processed to report the 'percent change of mean lacteal diameter.' The utility of expressing the percent change in mean lacteal diameter as opposed to absolute change lies in its ability to normalize for deviations in mean diameter across lacteals of varying sizes. The lacteal contraction was assessed by quantifying the percent deviation of lacteal diameter from the mean lacteal diameter over time in response to placebo or treatments.

Rat Fistula Model

Mesenteric lymph duct and duodenal cannulation. The mesenteric lymph duct and duodenum was cannulated under inhalant isoflurane anesthesia, as previously described.[6,17] Briefly, a polyvinyl chloride tubing (0.50 mm inside diameter; 0.80 mm outside diameter) was advanced into the mesenteric lymph duct and was secured by a drop of cyanoacrylate glue. Silicone tubing (1.02 mm inside diameter; 2.16 mm outside diameter) was advanced ∼1 cm into the duodenum via a fundal incision in the stomach, which was secured by a purse-string suture. Preoperative buprenorphine 0.05 mg/kg and meloxicam 0.1 mg/kg was provided as systemic analgesics and lidocaine 2% (0.05 mL) and bupivacaine 0.25% (0.05 mL) were used as local analgesics (Figure 1B). After surgery, rats were housed in a Bollman restraint cage with ambient temperature maintained at 26 °C using heating pads under and around the cage to support thermoregulation. Immediately after surgery, an intraduodenal infusion of normal saline containing 5% glucose was commenced at a rate of 3 mL/h for 5 hours. To simulate an overnight fast, normal saline without glucose was infused intraduodenal at a rate of 3 mL/h and was continued throughout the remainder of the study.

Pharmacological treatments and lymph fluid collection. As shown in Figure 1B, after an overnight fast with intraduodenal saline infusion (3 mL/h), rats received an intraduodenal lipid bolus of 1.5 ml 20% Intralipid (Sigma Aldrich, St. Louis, MO) chased by 0.5 mL saline (as represented

by a yellow arrow in Figure 1B). Continuous intraduodenal saline infusion of 3 mL/h was continued for the duration of the study. At 300 minutes (5 hours) post lipid bolus, rats were randomly assigned to receive 1 intraduodenal treatment. Sprague–Dawley rats received 1 of the 4 treatments (red arrow): (1) Placebo (1 mL of 0.9% saline); (2) GLP-2 (75 μg GLP-2 in 0.5 mL PBS); and (3) GLP-2 (75 μg GLP-2 in 0.5 mL PBS) + MEC (10 mg/kg). n = 8 rats were used for each group. The indicating reagents were pushed into the duodenum by using a syringe within seconds, separate from the saline (3 mL/h speed). Lymph samples were then collected on ice for 1 hour following treatments, beginning with 5-minute intervals for 30 minutes and 15-minute intervals for the remaining time. Lymph fluid was collected by gravity, allowing continuous flow, and limiting the opportunity for clotting. Small clots within the tubing were extracted by mild suction with a syringe and had minimal impact on lymph flow. The collection of lymph fluid was conducted in awake rats. Rats were euthanized at 240 minutes post lipid bolus with pentobarbital overdose (80 mg/kg) at the end of the experiment. Lymph samples were frozen at −20 °C and analyzed for TG concentration and for apolipoprotein B48 content.

TG Assay

TG concentration was measured using a colorimetric assay kit (L-type Triglyceride M, Wako Diagnostics, Richmond, VA) following the manufacturer's instructions. Briefly, lymph flow samples were diluted 5 times, 10 μL of the diluted sample was added to a 96-well plate followed by the reagents from the assay kit. The absorbance of each well at 600 nm was measured by Opsys MR Microplate Reader (DYNEX Technologies, Inc, Chantilly VA) and TG concentration was calculated using the manufacturer's instructions.

Calculations and Statistical Analysis

Triglyceride output (mg/h) was calculated as the product of lymph flow (mL/h) and TG concentration (mg/mL). All the statistical analyses were performed using GraphPad Prism Software (version 10.0.0 [153], GraphPad Software, Boston, MA). Data are presented as means ± standard error of the mean. First, outliers were identified using the Robust regression method. If the outliers were present, then the statistical analysis was repeated with and without the outlier(s). No differences were observed for the statistical significance (with or without an outlier); thus, the data including outliers were presented in the manuscript. For the variables with repeated measurements (lacteal contractility, lymph flow, TG concentration, TG output, cumulative lymph volume, and cumulative TG mass), outliers were identified using visualizing data using box plots, sphericity was not assumed, and thus, a Geisser-Greenhouse's correction (ε) was used in the analysis and epsilon values were presented in the figures wherever applicable. These variables were analyzed by using repeated measure analysis of variance or mixed-effects analysis (restricted maximum likelihood), in case if missing values were present. The measurements at different time points were considered repeated measures, treatment (placebo, GLP-2, and GLP-2 + MEC) was used as a between-group factor, and time was used as a within-group factor. Data are presented as mean ± standard error of the mean. Statistical significance was declared at $P \leq .05$. Finally, due to the novelty of these findings, we have explored alternative ways to analyze our data so as to be confident of our findings. Therefore, we have consulted Drs Kumar Murty and Justin Trent, mathematicians from the Fields Institute for Research in Mathematical Sciences, Toronto, ON. From each 30-second video, 60 data points were collected for each line profile. From 5-line profiles, a total of 300 data points (representing lacteal diameter) were recorded. Blinded raw data from all time points were used by the statisticians, and the percent change in mean lacteal diameter was calculated. Data points falling within the mean ± standard deviation (SD) were considered as normal lacteal diameter. If the data points were under the range of mean ± 2SD, these data points were considered as lacteals with wide/narrow diameter, and lastly, if the data points were under the range of mean ± 3SD, these data points were considered as lacteals with extremely wide/narrow diameter. Data presented here were the proportion of data points (in percentage) for each category; thus, no statistical analysis was performed for these data.

Results

Lacteal Contractility

Shown in Supplementary Video 1 is the real-time recording capturing the dynamics of lacteal contractility immediately following GLP-2 administration (0 minute) and at the 15-minute post–GLP-2 administration. GLP-2 treatment resulted in an average of up to 27% change in lacteal diameter at 15 minutes (at 0 minute was up to 3%), as opposed to 3% (0 minute: 3%) and 2% (0 minute: 1%) change in response to placebo and MEC treatments, respectively. As shown in Figure 2A, compared to baseline measurements (0 minute), lacteal contractility (measured as the standard deviation [n = 8 per group] of lacteal diameter over a 30-second period) peaked at 15 minutes in response to GLP-2 ($P < .05$, central panel). By 30 minutes, lymphatic contractility had returned to baseline values ($P > .05$). Interestingly, in response to ENS inhibition (via MEC), GLP-2-induced enhancement of lacteal contractility was significantly inhibited (as represented by no significant change in lacteal contractility at all time points: −3 minutes to 30 minutes). Shown in Figure 2B is the analysis of the data using a different statistical technique. At time −3 minutes, in response to GLP-2, almost all the data points (∼95%) were within 'normal range' (ie, <2SD from the mean lacteal diameter), indicating lacteal diameter did not change during a 30-sec video at −3 min (consistent with Figure 2A), which is the baseline unstimulated lymphatic contractility. Over time, within 5–10 minutes, >20% of the data points shifted into either narrow/wide or extremely narrow/wide categories, and by 15 and 20 minutes, 49% and 24% of data points, respectively, were in the extremely narrow or wide range suggesting increased lacteal contractility in response to GLP-2. By 30 minutes, 89% of the data points had returned to the normal range. To visually compare changes in lacteal contractility, we recorded the variance of percent change in lacteal diameter from each time point and performed mixed-model analysis (restricted maximum likelihood). As represented in Figure 3, a significant increase in

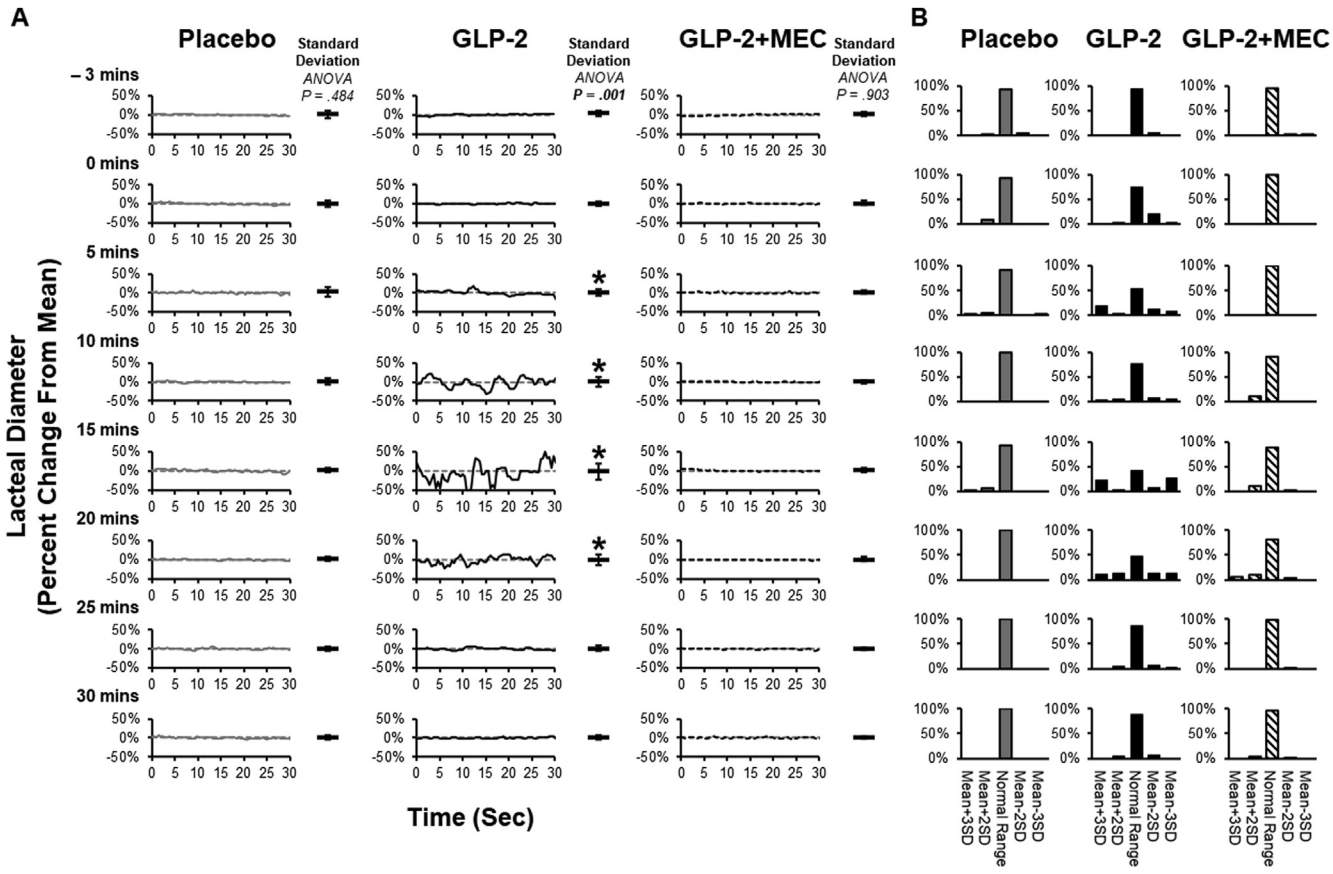

Figure 2. Enhancement of lacteal contractility in response to GLP-2 via ENS. Data are represented in percent change relative to mean lacteal diameter (represented as 0% on y-axis). n = 8 animals per group. (A) Representative figure from each group (PLC: animal #6, GLP-2: animal #7, and GLP-2 + MEC: animal #4) for percent change in lacteal diameter recorded over 30 seconds at each time point. Variance presented next to each line graph corresponds to the standard deviation (variance) in lacteal diameter calculated from all animals' average data. *$P \leq .05$ compared to 0 minute time point. (B) An alternate approach (mathematician's approach) to quantify changes in lacteal contractility in response to different treatments. No statistical analysis was performed for (B). GLP-2, glucagon-like peptide 2; MEC, mecamylamine.

the variability of mean lacteal diameter was observed by 10–20 minutes, peaking at 15 minutes (3-fold increase) in response to GLP-2, demonstrating that lacteal diameter changed significantly, compared to baseline (0 minute). By 30 minutes, the variance had returned to the baseline value or resting state. Interestingly, the inhibition of ENS completely reversed the effect of GLP-2-induced enhancement of lacteal contractility ($P > .05$).

Lymph Flow Dynamics

As shown in Figure 4A, lymph flow significantly increased in response to GLP-2 compared to the placebo group peaking at 10 minutes time point (*$P < .05$ for all within-group effect; #$P < .05$ compared to the placebo group at respective time point for all between-group effect). When ENS inhibitor was coadministered, GLP-2 enhancement of lymph flow was significantly inhibited with no differences between GLP-2 + MEC and placebo group ($P < .001$ compared to GLP-2 and $P = .534$ compared to placebo as depicted for area under the curve [AUC] in the bar graphs). Similarly, cumulative lymph volume was also significantly increased with all treatments; however, the increase with GLP-2 treatment was at least 2-fold higher than the placebo group (*$P < .05$ for all within-group effect; #$P < .05$ compared to the placebo group at respective time point for all between-group effect). This increase in cumulative lymph volume was significantly inhibited when the ENS inhibitor was coadministered ($P < .001$ compared to GLP-2 as depicted in AUC bar graphs of Figure 4B).

TG and CM Metabolism

With regard to TG output (Figure 4C), which is a product of lymph flow and TG concentration, GLP-2 increased TG output significantly, peaking at 10 minutes (*$P < .05$ for all within-group effect; #$P < .05$ compared to placebo group at respective time point for all between-group effect). In contrast, coadministration of ENS inhibitor significantly blunted the effect of GLP-2 on TG or CM output ($P = .001$ compared to the GLP-2 group as depicted in AUC bar graphs). Interestingly, the reduction in TG output or CM

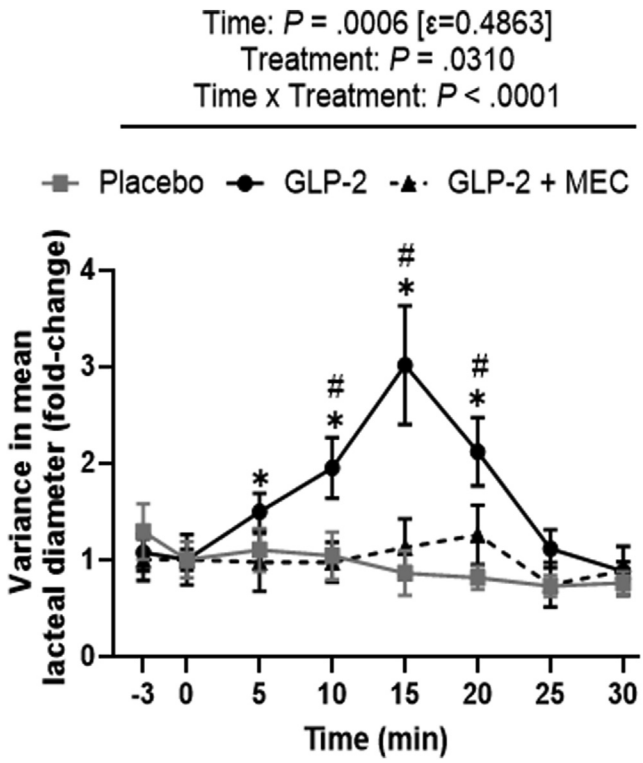

Figure 3. Lacteal contractility in response to treatments. Data are represented in mean ± standard error. n = 8 animals per group. Fold-change in lacteal variance was calculated based on time point 0 min (represented as 1 on y-axis). One data point (15 minutes time point) for 1 rat was missed due to technical issue during recording of live videos. Therefore, mixed-effects analysis (RELM) was performed instead of 2-way ANOVA. Dunnett's multiple comparisons test was performed for post-hoc analysis. *$P \leq .05$ compared to 0 minute (within-group analysis). #$P \leq .05$ compared to placebo at same time point (between-group analysis). GLP-2, glucagon-like peptide 2; MEC, mecamylamine; ANOVA, analysis of variance.

secretion was to the extent that the values at certain times were significantly lower than the placebo group (#$P < .05$ for all points).

Correlation Between 2 Models

Based on the data presented, the lacteal contractility timeline (Figure 3) was superimposable with the timeline of lymph flow (Figure 4A) and TG output data (Figure 4C). Therefore, we performed a linear regression model analysis among lacteal contractility, lymph flow, and TG output for all the groups. Indeed, as shown in Figure 5A and B, a significant relationship was found between change in lacteal diameter (fold-change) and lymph flow ($P < .0001$, $R^2 = 0.613$), indicating an increase in lymph flow was associated with increased lacteal contractility. A similar relationship was observed between change in lacteal diameter and TG output ($P = .0018$, $R^2 = 0.409$), indicating an increase in TG output was associated with increased lacteal contractility.

Discussion

The intricate interplay among gut peptides, lipoprotein metabolism, and the ENS has been a relatively unexplored area in gastrointestinal physiology.[3] Previous studies from our research group have shown that GLP-2 exerts its lipid-mobilizing effects distal to the Golgi apparatus, significantly enhancing the output of preformed CMs rather than affecting cytoplasmic lipid droplets or the size of CMs.[4–7,10]

GLP-2 is an intestinotrophic peptide that specifically binds to its cognate G protein-coupled receptor (GLP-2R) and exerts its effects on various physiological functions including lymphatics.[18] In addition to smooth muscle cells surrounding lacteals,[19] GLP-2Rs are present on the vagal afferent neurons, on the enteric nerves, and on the telocytes that were adjacent to epithelial stromal cells.[11,12,20] Specifically, GLP-2Rs were identified on the ganglion of nerves innervating the myenteric and submucosal plexus, with GLP-2R-positive neurons comprising both excitatory and inhibitory types. While interstitial cells of Cajal lacked GLP-2R expression, they were enclosed by GLP-2R-positive nerve varicosities coexpressing excitatory or inhibitory neurotransmitters. These varicosities were primarily found on excitatory pathways, with a predominant presence of GLP-2R on them.[21,22] In a recent study, Mukherjee et al[23] vagotomized rats (blocked vagal nerve) to understand the role of the parasympathetic nervous system on lymphatic pumping and lipid mobilization, and reported a partial inhibition of GLP-2-induced lymph flow (a surrogate marker of lacteal contractility[24]), lymph volume, and TG output. These findings were expected since vagotomy in dogs has previously been shown to reduce villus motility by 20%.[13] Moreover, from recent understanding of ENS studies, vagal innervation of the small intestine does not appear to be the primary regulator of intestinal function (eg, intestinal motility, digestion, and gut responses), as opposed to traditional belief (as reviewed by Sharkey and Mawe[25]). Rather ENS appears to self-regulate intestinal function (eg, muscle activity and motility, fluid fluxes, mucosal blood flow, and also mucosal barrier function[26]) through signals from other enteric neurons and local circuits, independent of signaling from central or autonomic nervous system[26] (few preganglionic vagal innervations in the myenteric ganglia[27]), albeit few excitatory nerve innervations from sympathetic nervous system into blood vessel and sphincters.[28,29] Thus, the observed inability of vagotomy to fully inhibit the GLP-2-induced enhancement of lymph dynamics and TG output in the study by Mukherjee et al[23] strongly suggests that these processes are primarily driven by the ENS and potentially autonomic nervous system. Therefore, we postulated that GLP-2 may be exerting its intestinal lipid mobilization effect by acting through the predominant mechanism of excitatory neurotransmission of the ENS and autonomic nervous system.

To study the role of ENS on lymphatics dynamics and lipid mobilization, we used a ganglion-blocking agent (MEC, which nonselectively blocks nicotinic acetylcholine

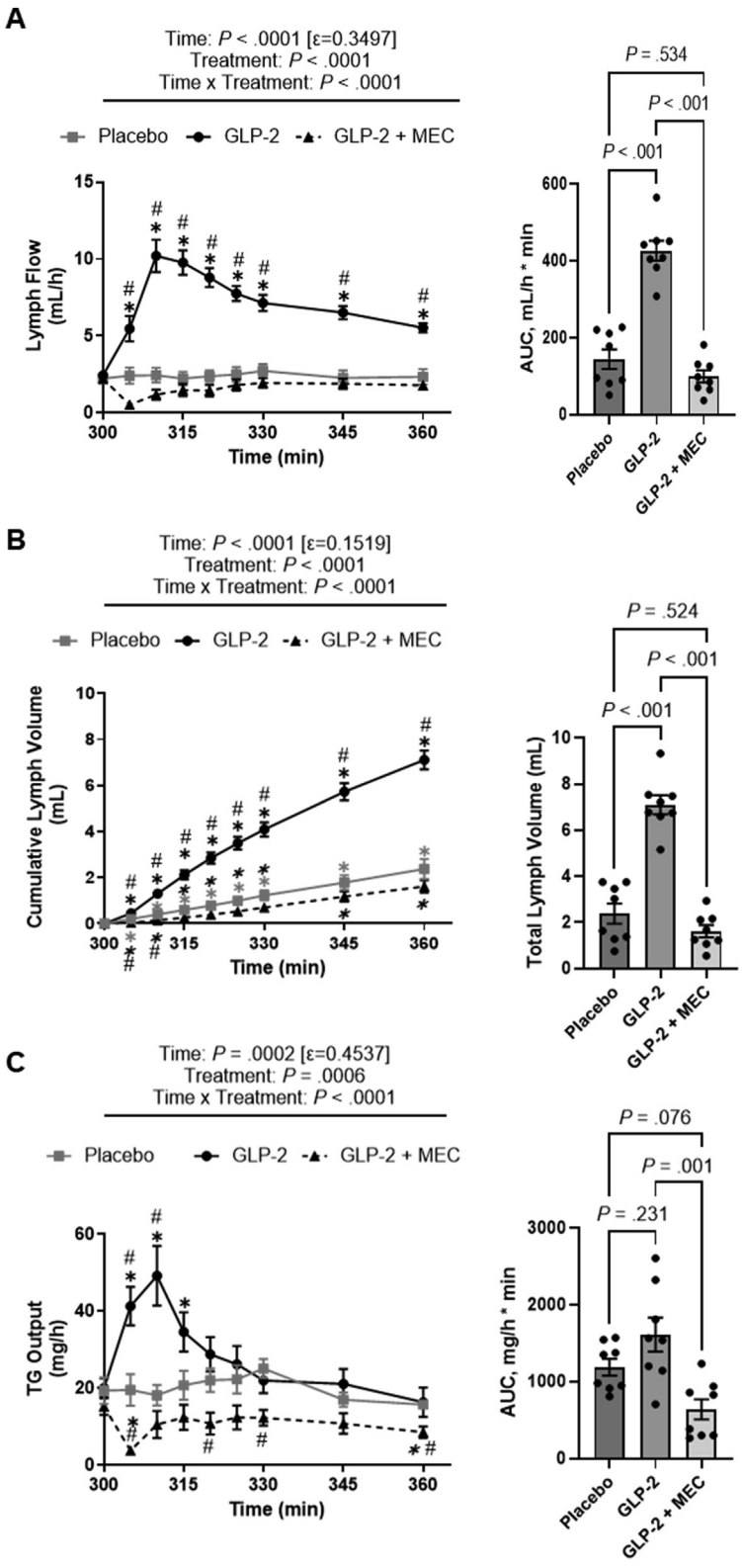

Figure 4. Lymph dynamics and intestinal lipid mobilization in response to treatments. Data are represented in mean ± SE. n = 8 animals per group. Absolute changes in lymph flow (A), cumulative lymph volume (B), and TG output (C), in response to treatment were reported. For line graphs, 2-way repeated measure ANOVA with Dunnett's multiple comparisons test (if significant) was performed. For bar graphs, 1-way ANOVA with Bonferroni post hoc test (if significant) was performed. *$P \leq .05$, compared to 300 minutes (within-group analysis). #$P \leq .05$, compared to placebo at same time point (between-group analysis). ANOVA, analysis of variance; GLP-2, glucagon-like peptide 2; MEC, mecamylamine; TG, triglycerides.

receptor-mediated neurotransmission) along with GLP-2. In addition to lymph dynamics, in the present study, to the best of our knowledge, for the first time, we directly quantified lacteal contractility in a Prox-1-EGFP transgenic rat model using intravital fluorescence imaging. Consistent with our previous hypothesis, GLP-2 significantly increased lacteal contractility compared to placebo treatment, and the time course of this enhancement in lacteal contractility was concordant with the increase in lymph flow and lymph TG output, as determined in the rat lymph fistula model (with

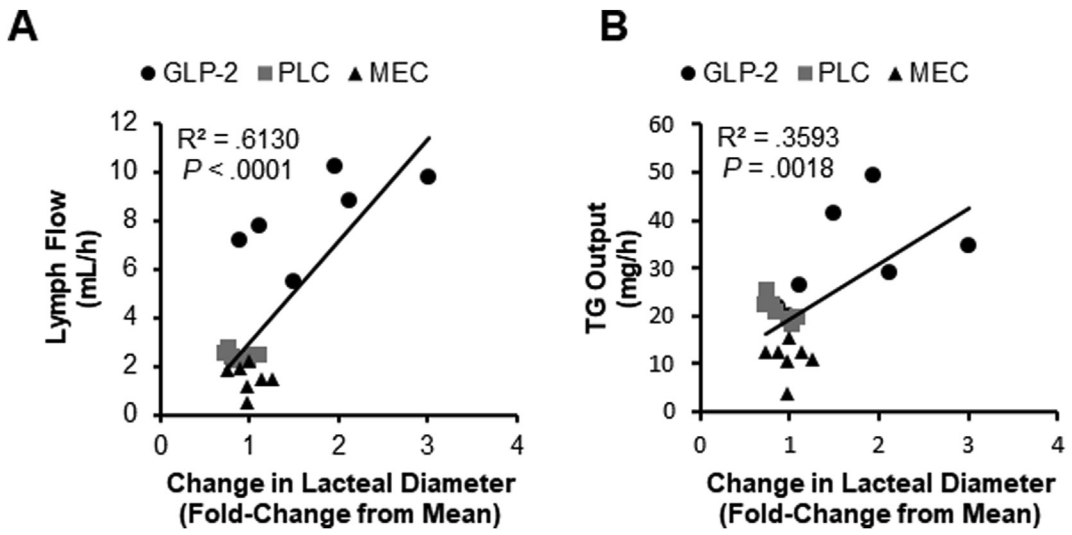

Figure 5. Relationship between lacteal contractility and lymph flow and TG output. n = 8 animals per group. Data points from all 24 animals (3 groups) were used to evaluate a relationship among lacteal contractility, lymph flow, and TG output. (A) A grouped correlation analysis between change in lacteal diameter (fold-change from the mean lacteal diameter) and lymph flow. (B) A grouped correlation analysis between change in lacteal diameter (fold-change from the mean lacteal diameter) and TG output. A linear regression model analysis was performed where change in lacteal diameter was considered as an independent variable and lymph flow, and TG output was considered as a dependent variable. TG, triglycerides.

peak enhancement at approximately 15 minutes). When MEC was administered along with GLP-2, the GLP-2-induced enhancement of lacteal contractility was completely abolished in the present study. The amplitude and frequency of contractions were similar to a previously published study, in which lymphatic pumping was recorded at a single time point in response to known enhancers (eg, acetylcholine) of lymphatic pumping.[14]

Although both sympathetic and parasympathetic nervous systems regulate villus contractility, based on our findings and previous literature, ENS regulation of lacteal contractility appears to be a predominant factor.[25] In the present study, we showed that GLP-2's enhancement of lacteal contractility was primarily regulated through the ENS. We did not conduct experiments involving vagotomy or complete blockade of ENS through tetrodotoxin (block action potential generation and propagation by binding to a voltage-gated sodium channel). Although tetrodotoxin may serve as a tool to completely block ENS, it may result in the blockade of both the stimulation and inhibition of lacteal contraction, thus resulting in no differences in lacteal contractility.[14]

In parallel to the intravital imaging studies that examined lacteal contractility, in a separate group of rats, we examined the effect of GLP-2-induced enhancement of lacteal contractility on the actual lymph flow of intestinal lipids and assessed the role of the ENS in modulating this effect. Using a rat lymphatic fistula model in Sprague–Dawley rats, consistent with our previous work,[5–7,10] we reported a rapid and robust enhancement of lymph flow and cumulative lymph volume over 30 minutes, TG output, and cumulative TG mass in response to intraperitoneal GLP-2 administration. Importantly, inhibition of the ENS completely blocked GLP-2-induced enhancement of lymph flow, lymph volume, and cumulative lymph volume. Similarly, TG output and cumulative TG mass were significantly reversed with the coadministration of GLP-2 and MEC when compared to GLP-2 alone. These findings may indicate that GLP-2 is signaling lacteal contractility by stimulating the ENS, perhaps via a neurotransmitter, or alternatively that intact ENS is absolutely required for other GLP-2-stimulated signals to enhance lacteal contractility. Future studies will need to address this important question. Previous studies[14,30–32] administered MEC directly on the small intestine (luminal administration), rather than intravenous or intraperitoneal administration, to study ENS effects as opposed to central effects (combined ENS and potentially autonomic nervous system). However, in our experiments from rat fistula studies, we did not observe any significant differences between intraperitoneal (Figure 4) and intraduodenal (Figure A3) administration of MEC on all the parameters of lymph dynamics and TG output, suggesting that the local effects of blocking the autonomic nervous system with intraduodenal MEC may not significantly alter these specific lymphatic processes within the duodenal region, potentially indicating a predominant influence of the ENS or complex interplays of regulatory mechanisms in the observed outcomes.

Interestingly, in view of the significant increase in amplitude and frequency of lacteal contractions demonstrated here, which confirms that GLP-2 enhances lymphatic contractility, the time course of GLP-2-induced lacteal contractility as shown in Figure 3 is virtually superimposable on the time course of TG-output data from the rat

lymph fistula model (Figure 4C), both increasing to a maximum at 10–15 minutes post GLP-2 administration, before returning toward baseline. These data highly suggest, but do not prove, the cause and effect between stimulation of lymphatic contractility and lymphatic TG output. This finding is also consistent with our own previous work, in animals and humans, that has strongly suggested that GLP-2, the most potent mobilizer of gut lipid and CM secretion in our hands, does not require the canonical CM synthetic pathway and acts beyond the enterocyte.[7] This is the first proof-of-principle demonstration that enhancement of lymphatic contractility plays a regulatory role in CM secretion, and it opens the field to exploring new treatments for hyperlipidemia and the prevention of metabolic diseases.

The imperative for employing intravital imaging, exemplified in experiments using Prox-1-EGFP rats to study lacteal contractility in response to GLP-2, becomes particularly relevant in the context of our findings. The inherent limitation of the rat fistula model, incapable of measuring dynamic lymphatic pumping, underscores the necessity of intravital imaging as the indispensable method for quantitatively assessing lacteal contractility in real-time and in vivo within the physiological context of living organisms. While previous study[14] used whole-area lacteal diameter for contractility quantification, our methodology rigorously monitored lacteal diameter changes while systematically excluding potential artifacts. Specifically, we employed several measures to control for artifacts. Tissue penetration was avoided by maintaining a minimum lens-to-tissue working distance of 1.7 mm, effectively minimizing undulating lacteal contractions. Furthermore, we opted for a transgenic rat model to control for imaging intensity, thereby preventing the common issue of intensity degradation associated with imaging dye administration. Additionally, to rectify tissue motion, we drew line profiles crossing both background and lacteal regions. Finally, in our preliminary experiments, superficial administration of treatments resulted in increased motility of the tissue, potentially due to increased smooth muscle contraction, resulting in loss of the target lacteal from the imaging area. Moreover, owing to the 3-dimensional nature of smooth muscle contractions, discerning whether the observed changes in lacteal diameter were attributable to genuine lacteal contraction or merely z-axis displacement of the imaged plane proved challenging. Therefore, intraperitoneal administration of the treatments prevented excessive tissue motility and provided us confidence that observed changes in lacteal diameter were likely due to increased lacteal contractility. This critical methodological adaptation allowed us to unveil the regulatory role of lacteal contractility in CM secretion, providing novel insights that enhance our understanding of the interplay among gut peptides, lipoprotein metabolism, and the ENS.

Conclusion

In this study, we investigated the interplay among gut peptides, lipoprotein metabolism, and the ENS. Our findings show for the first time that regulation of lymphatic contractility is a critical site of regulation of CM transport to the blood circulation. The gut peptide GLP-2 enhances lacteal contractility and CM transport through increased lymphatic pumping. Notably, the ENS plays a crucial role in mediating this effect, as blocking ganglion-mediated neurotransmission completely negated GLP-2's impact on lacteal contractility. These findings prove our previous hypothesis that GLP-2 acts beyond the enterocyte in regulating intestinal lipid transport. In addition to providing new insights into GLP-2's impact on lacteal contractility and gut lipid mobilization, this study also enhances our general understanding of the regulation of CM transport from the intestine to the blood circulation, providing potential therapeutic applications in hyperlipidemia and metabolic disorders and advancing the field of gastrointestinal physiology.

Supplementary Materials

Material associated with this article can be found, in the online version, at https://doi.org/10.1016/j.gastha.2024.06.009.

References

1. Ginsberg HN, Packard CJ, Chapman MJ, et al. Triglyceride-rich lipoproteins and their remnants: metabolic insights, role in atherosclerotic cardiovascular disease, and emerging therapeutic strategies-a consensus statement from the European Atherosclerosis Society. Eur Heart J 2021;42:4791–4806.
2. Stahel P, Xiao C, Nahmias A, et al. Multi-organ coordination of lipoprotein secretion by hormones, nutrients and neural networks. Endocr Rev 2021;42:815–838.
3. Syed-Abdul MM, Tian L, Xiao C, et al. Lymphatics - not just a chylomicron conduit. Curr Opin Lipidol 2022;33:175–184.
4. Dash S, Xiao C, Morgantini C, et al. Glucagon-like peptide-2 regulates release of chylomicrons from the intestine. Gastroenterology 2014;147:1275–1284.e4.
5. Xiao C, Stahel P, Morgantini C, et al. Glucagon-like peptide-2 mobilizes lipids from the intestine by a systemic nitric oxide-independent mechanism. Diabetes Obes Metab 2019;21:2535–2541.
6. Stahel P, Xiao C, Davis X, et al. Glucose and GLP-2 (glucagon-like peptide-2) mobilize intestinal triglyceride by distinct mechanisms. Arterioscler Thromb Vasc Biol 2019;39:1565–1573.
7. Syed-Abdul MM, Stahel P, Tian L, et al. Glucagon-like peptide-2 mobilization of intestinal lipid does not require canonical enterocyte chylomicron synthetic machinery. Biochim Biophys Acta Mol Cell Biol Lipids 2022;1867:159194.
8. Hsieh J, Trajcevski KE, Farr SL, et al. Glucagon-like peptide 2 (GLP-2) stimulates postprandial chylomicron production and postabsorptive release of intestinal triglyceride storage pools via induction of nitric oxide signaling in male hamsters and mice. Endocrinology 2015;156:3538–3547.

9. Grande EM, Raka F, Hoffman S, et al. GLP-2 regulation of dietary fat absorption and intestinal chylomicron production via neuronal nitric oxide synthase (nNOS) signaling. Diabetes 2022;71:1388–1399.
10. Syed-Abdul MM, Stahel P, Zembroski A, et al. Glucagon-like peptide-2 acutely enhances chylomicron secretion in humans without mobilizing cytoplasmic lipid droplets. J Clin Endocrinol Metab 2023;108:1084–1092.
11. Guan X, Karpen HE, Stephens J, et al. GLP-2 receptor localizes to enteric neurons and endocrine cells expressing vasoactive peptides and mediates increased blood flow. Gastroenterology 2006;130:150–164.
12. Nelson DW, Sharp JW, Brownfield MS, et al. Localization and activation of glucagon-like peptide-2 receptors on vagal afferents in the rat. Endocrinology 2007; 148:1954–1962.
13. Womack WA, Mailman D, Kvietys PR, et al. Neurohumoral control of villous motility. Am J Physiol 1988; 255:G162–G167.
14. Choe K, Jang JY, Park I, et al. Intravital imaging of intestinal lacteals unveils lipid drainage through contractility. J Clin Invest 2015;125:4042–4052.
15. Jung E, Gardner D, Choi D, et al. Development and characterization of a novel Prox1-EGFP lymphatic and Schlemm's canal reporter rat. Sci Rep 2017;7:5577.
16. Coste A, Oktay MH, Condeelis JS, et al. Intravital imaging techniques for biomedical and clinical research. Cytometry 2020;97:448–457.
17. Tian L, Syed-Abdul MM, Stahel P, et al. Enteral glucose, absorbed and metabolized, potently enhances mesenteric lymph flow in chow and high fat fed rats. Am J Physiol Gastrointest Liver Physiol 2022;323:G331–G340.
18. Estall JL, Drucker DJ. Glucagon-like peptide-2. Annu Rev Nutr 2006;26:391–411.
19. Orskov C, Hartmann B, Poulsen SS, et al. GLP-2 stimulates colonic growth via KGF, released by subepithelial myofibroblasts with GLP-2 receptors. Regul Pept 2005; 124:105–112.
20. Zhu G, Lahori D, Schug J, et al. Villification of the intestinal epithelium is driven by Foxl1. bioRxiv 2024. http://doi.org/10.1101/2024.02.27.582300.
21. Cinci L, Faussone-Pellegrini MS, Rotondo A, et al. GLP-2 receptor expression in excitatory and inhibitory enteric neurons and its role in mouse duodenum contractility. Neuro Gastroenterol Motil 2011;23:e383–e392.
22. Yusta B, Matthews D, Koehler JA, et al. Localization of glucagon-like peptide-2 receptor expression in the mouse. Endocrinology 2019;160:1950–1963.
23. Mukherjee K, Wang R, Xiao C. Release of lipids stored in the intestine by glucagon-like peptide-2 involves a gut-brain neural pathway. Arterioscler Thromb Vasc Biol 2024;44:192–201.
24. Womack WA, Tygart PK, Mailman D, et al. Villous motility: relationship to lymph flow and blood flow in the dog jejunum. Gastroenterology 1988;94:977–983.
25. Sharkey KA, Mawe GM. The enteric nervous system. Physiol Rev 2023;103:1487–1564.
26. Breit S, Kupferberg A, Rogler G, et al. Vagus nerve as modulator of the brain-gut axis in psychiatric and inflammatory disorders. Front Psychiatry 2018;9:44.
27. Holst MC, Kelly JB, Powley TL. Vagal preganglionic projections to the enteric nervous system characterized with Phaseolus vulgaris-leucoagglutinin. J Comp Neurol 1997;381:81–100.
28. Lomax AE, Sharkey KA, Furness JB. The participation of the sympathetic innervation of the gastrointestinal tract in disease states. Neuro Gastroenterol Motil 2010;22:7–18.
29. McIntyre AS, Thompson DG. Review article: adrenergic control of motor and secretory function in the gastrointestinal tract. Aliment Pharmacol Ther 1992;6:125–142.
30. Obaid AL, Nelson ME, Lindstrom J, et al. Optical studies of nicotinic acetylcholine receptor subtypes in the Guinea-pig enteric nervous system. J Exp Biol 2005; 208:2981–3001.
31. Dahlgren D, Roos C, Lundqvist A, et al. Time-dependent effects on small intestinal transport by absorption-modifying excipients. Eur J Pharm Biopharm 2018; 132:19–28.
32. Dahlgren D, Roos C, Lundqvist A, et al. Effect of absorption-modifying excipients, hypotonicity, and enteric neural activity in an in vivo model for small intestinal transport. Int J Pharm 2018;549:239–248.

Received April 29, 2024. Accepted June 24, 2024.

Correspondence:
Address correspondence to: Gary F. Lewis, MD, Toronto General Hospital, 200 Elizabeth St, EN12-244, Toronto, Ontario M5G2C3, Canada. e-mail: Gary.Lewis@uhn.ca.

Acknowledgments:
The authors acknowledge the support of the Advanced Optical Microscopy Facility (AOMF) for intravital imaging, the Animal Resources Centre (ARC) for their help with breeding Prox-1-EGFP rat model and maintaining of Sprague–Dawley rats. The authors would also like to acknowledge Drs Kumar Murty and Justin Trent, mathematicians from the Fields Institute for Research in Mathematical Sciences, Toronto, ON, Canada, for their input on data analysis for lacteal contractility.

Authors' Contributions:
Majid Mufaqam Syed-Abdul: Conceptualization, methodology, formal analysis, investigation, data curation, writing – original draft, writing – review and editing, visualization, and project administration. Lili Tian: Conceptualization, methodology, investigation, data curation, writing – review and editing, and project administration. Gary F. Lewis: Conceptualization, methodology, software, validation, investigation, resources, writing – review and editing, supervision, and funding acquisition. Timothy Samuel: Methodology, software development, writing – review and editing, and project administration. Ralph S. Dacosta: Methodology, validation, writing – review and editing, and supervision. Alex Wong: Writing – review and editing. Young-Kwon Hong: Writing – review and editing.

Conflicts of interest:
The authors disclose no conflicts.

Funding:
G.F.L. holds the Drucker Family Chair in Diabetes Research, and this work was funded by an operating grant from CIHR (PJT-153301). M.M.S.-A. is a recipient of the Banting and Best Diabetes Centre Postdoctoral Fellowship (2022–2023) and the CIHR Postdoctoral Fellowship (MFE-187912, 2023–2026) awards.

Ethical Statement:
All the animals were treated ethically, and all the protocols and procedures were approved by the University Health Network Animal Care Committee (Approval nos. 5690 and 6211).

Data Transparency Statement:
Data, analytic methods, and study materials can be made available upon a reasonable request to corresponding author.

Reporting Guidelines:
ARRIVE.